MULTISCIA
JOURNALS PUBLISHERS

FRONTIERS IN PHARMACEUTICS

ISSN: (3065- 1786)

editor.fpm1@gmail.com

https://multisciajournals.com/journals/index.php/fp

Frontiers in Pharmaceutics
Volume 1 Issue 2 2025

PLGA Microspheres' Association with Carrier Pellets by Fluid Bed Coating: An Innovative Method for Increasing Microparticle Flowability

KH Yang, HT Peng,
Department of **Pharmaceutics**

Article Info

Received: 28-04-2025 Revised:08-05-2025 Accepted:14-05-2025 Published:25-05-2025

1. Introduction

Because of their potential biopharmaceutical benefits, micro- and nanoparticles have been investigated as possible oral drug delivery methods. These systems may improve drug absorption [1] and regulate drug release [2] according to their granulometric profiles and chemical compositions. Additionally, the micro- and nanoencapsulation of bioactive substances may result in an overall improvement in medication stability [3, 4]. However, because of their small particle size, these systems have significant technical restrictions that result in decreased flowability in the solid state. Managing and processing such tiny particles could turn into a significant industrial issue because of their compromised mechanical qualities [5], which affects the viability and cost of manufacture.

A number of particle properties, including surface chemistry, texture, contact area, particle density, and hygroscopicity, can influence powder flow. Adhesion forces, such as capillary, Van der Waals, and electrostatic forces, may therefore exert a greater influence on the particles. This is particularly true for particles that are extremely susceptible to interparticle forces and have an average diameter of less than 10 m [6, 7]. These systems have a large surface area because of their smaller particle size, which increases the contact surface between each individual particle and promotes interparticle interactions [7]. Consequently, the net adhesion between particles of

flowability decreases as the system grows [8]. Conversely, for larger particles, powders can flow freely because gravitational forces are stronger than interparticle forces [8].

Because of this, industrial scientists are always looking for ways to make micro and submicrometric particles more flowable. The attachment of micro/nanoparticles to carrier particles is among the most promising tactics. There has been a discernible rise in patent applications over the past ten years that suggest solutions to this problem. Patents from companies like 3M Innovative Properties, Co. [9], Applied Nanotech Holdings, Inc. [10], Universidad Nacional Autonomous de Mexico [11], Evonik Rohm Gmbh. [12], and Teva Pharmaceutical Industries, Ltd. [13] demonstrate this.

In order to improve the mechanical qualities of the finished product, we present a novel, standardized methodology in this work that links poorly flowing particles to macrostructures. Because of their poor flow characteristics, poly(lactic-co-glycolic acid) (PLGA) microspheres with a particle size of 10 m were selected as model particles. Because of its strong hygroscopicity, which increases the capillary forces acting on the particles loading it, Cecropia glaziovii freeze-dried extract was used as a model drug [14]. As a highly bioactive vegetal species [15–19], C. glaziovii has already been investigated as a bioactive product for use in medicine [20, 21]. Two hydrophilic polymers (Kollidon® VA64 and Kollicoat® Protect) were evaluated as coating materials to adhere microspheres to the surface of carrier pellets in the coating

investigations. Since these polymers are already used as components in other FDA-approved medications, their safety and quick dissolution made them the choice. Additionally, RGB (Red, Green, and Blue) image analysis [22] is suggested as a novel and affordable way to assess the pellets' entire covered surface. As illustrated in Figure 1, the process under investigation involved the use of top-spray fluid bed equipment to atomize and deposit microspheres on the surface of carrier pellets. When the dried polymeric covering came into contact with an aqueous media, the microspheres that were uniformly distributed throughout the intended structure easily disintegrated.

2. Supplies and Procedures

2.1. Supplies. Sigma-Aldrich (USA) and Vetec (Brazil) were the suppliers of polyvinyl alcohol and methylene blue, respectively. Boehringer Ingelheim (Germany) provided Poly(lactic-co-glycolic acid) (PLGA) 503H (50:50 lactic to glycolic acid ratio). BASF (Germany) generously donated Kollidon® VA64 (vinylpyrrolidone-vinyl acetate copolymer) and Kollicoat® Protect (polyvinyl alcohol-polyethylene glycol graft copolymer containing polyvinyl alcohol). Blanver (Brazil) contributed 101 commercially available microcrystalline cellulose pellets (average size of 1,000 m) made by extrusion-spheronization (Microcel® Pellets). The leaves of Cecropia glaziovii were acquired from the University of Campinas' Pluridisciplinary Center of Chemical, Biological, and Agronomic Studies in Brazil, and the freeze-dried extract used as the model medication was constructed in accordance with earlier literature descriptions [20]. Every other solvent and reagent was of analytical quality.

2.2. Making PLGA Microspheres Loaded with Cecropia Glaziovii Extract. The double emulsion solvent evaporation/extraction method was used to create microspheres loaded with Cecropia glaziovii extract. To create a water in oil emulsion (w1/o), 12.5 mg of freeze-dried extract was dissolved in 500 L of sodium hydroxide solution (0.5% w/v) and emulsified with 8 mL of PLGA 503H solution in dichloromethane (2.5 mg/mL) at 13500 rpm for two minutes (Ultra-Turrax® T25Basic, IKA, Germany; dispersing tool S25N-10G). To create a w1/o/w2 double emulsion, the emulsion was moved to 80 mL of a solution comprising polyvinyl alcohol (0.5% w/v) and sodium chloride (3% w/v) and emulsified at 13,500 rpm for 1 minute using the dispersing tool S20-25NK-19G. One hundred milliliters of a polyvinyl alcohol (0.1% w/v) and sodium chloride (3% w/v) solution were used to dilute the double emulsion. To allow the dichloromethane to evaporate and the microspheres to solidify, the final dispersion was agitated for two hours. To create a very hygroscopic dry powder, the solidified microspheres were centrifuged (RCF = 3256), rinsed three times with ultra-pure water, and freeze-dried (LD1500, Terroni, Brazil) for 48 hours.

2.3. Determining the parameters and coating variables. Kollidon® VA64 and Kollicoat® Protect are two hydrophilic polymers that were selected as coating materials for the coupling of microspheres to pellets. Using a top-spray fluid bed apparatus (Mini Coater Drier-2, Caleva, UK), some of the coating conditions were experimentally prestandardized. These included a 5 g batch, 13 Hz agitation, and an air inflow of 12.5 m3/s at 50°C. Methylene blue (0.01% w/v) was added to the polymer solution, and microspheres (5 mg/mL) were dissolved in it. At a rate of 1.5 mL/min, suspensions were atomized on the 1.5 bar pellet surface. After that, drying was done at 60°C for 10 minutes.

A IV-Optimal factorial design was used to assess three coating parameters (Table 1): (A) coating polymer type; (B) polymer concentration; and (C) coating suspension to pellets ratio (volume to weight). Consequently, a modified RGB image analysis method was used to determine total coated surface values [22]. A stereoscope (SZX16, Olympus, Brazil) was used to take pictures of 200 particles per formulation on a black glass surface in a controlled light condition at 25 lux (LightMeter, HS1010, China). ImageJ (1.45s, National Institutes of Health, USA) was used to process the photographs, and ColorInspector 3D (2.0, FHTW, Germany) was used to obtain color histograms. By comparing the RGB profile of uncoated pellets with the RGB frequencies per pixel, the total coated surface was calculated as a percentage. Pixels that were blue or white were categorized as "coated" or "uncoated," respectively.

The software Design-Expert® 8.0.7.1 (State-Ease Inc., USA) was used for regression analysis, and analysis

of variance (ANOVA) was used to determine the significance of single components, binary interactions, and quadratic factors ($p<0.05$).

TABLE 1: Experimental domain evaluated (IV-Optimal factorial design).

Factor	Levels		
	-1	0	+1
(A) Polymer type	Kollicoat® Protect	-	Kollidon® VA64
(B) Polymer concentration (% w/v)	1.0	2.5	5.0
(C) Coating suspension to pellets ratio (mL/g)	1:1	2:1	3:1

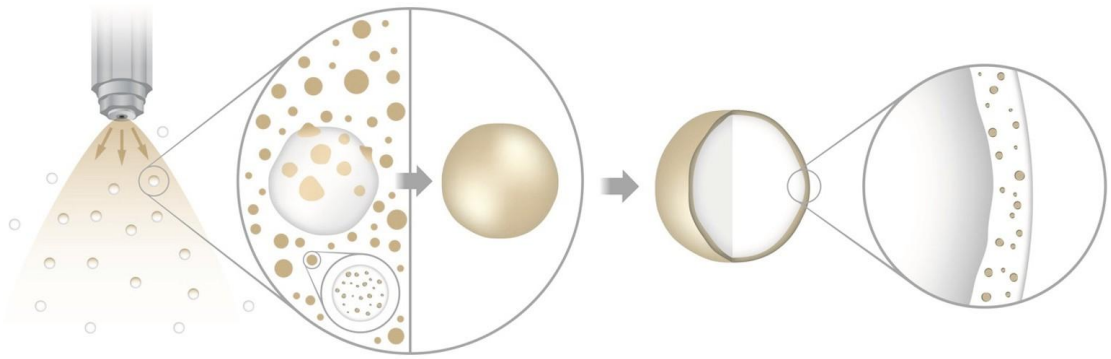

FIGURE 1: Schematic illustration of the preparation of microspheres-coated pellets by top-spray fluid bed coating.

1.1. Pellets coated with microspheres are prepared. As mentioned in Section 3.1 (Kollicoat® Protect 1.0% w/v at a 2:1 ratio of coating suspension to pellets), microspheres (5 mg/mL) were distributed in the coating polymer without the addition of methylene blue. Three 20 g batches (Mini Coater Drier-2, Caleva, UK) were made at 50°C with an air inlet of 14.0 m3/s and 13 Hz agitation. The pellets' surface was atomized with dispersions (1.5 bar, 1.5 mL/min), and then they were dried for 10 minutes at 60°C. Three coating layers were applied to each batch in order to theoretically reach a load of 30 mg of microspheres per g of pellets.

1.2. Determining Loading. K-Cell® chambers were used in a visual counting method to determine the microsphere burden.

2.7. Density and Flow Property Determination. Carr's index [14, 23], the Hausner ratio, and the static angle of repose [24] were used to determine the products' flow characteristics. A known mass of pellets was placed in a 100 mL cylinder, and the bulk density (b) was calculated as the mass to volume ratio. The mass to compressed volume ratio was calculated as the tapped density (t) after samples were put through 1250 taps using a tapped density tester (Copley JV1000, UK). The Hausner ratio (HR; (1)) and Carr's index (CI; (2)) were computed using both density values. Helium displacement pycnometry (AccuPycII 1340, Micromeritics Instrument Corp., USA) was used to determine the true density values at a helium flow of 2.2 kg/cm2. (Brazil, Intralab). For six hours, a known mass of pellets (n=3) was agitated by inversion (Tepron, Brazil) while dispersed in filtered water. 100 μL of the supernatant was later gathered.

1.3. Fourier Transform Infrared Spectroscopy with Attenuated Total Reflectance (ATR-FTIR). Using a scalpel, coating films were gently removed from the pellets' surface. A universal diamond ATR attachment connected to an FTIR spectrophotometer (Frontier, PerkinElmer, USA) was used to evaluate the samples directly. Analyses were conducted using a 4 cm−1 spectral resolution (32 scans/read) spanning the 4000–

600 cm−1 range.
The fixed-base piling method was used to calculate the static angle of repose [24]. A conical pile was created on the ground base by filling a suspended funnel (4 cm high) with samples and then releasing them. The angle of repose (n=6) was calculated from photos of the repose piles using a Size Meter 1.1, LCP/UFSC, Brazil.
2.8. Coated Pellets Cryosection. Using the microtome-cryostat CM1850UV (Leica Microsystems, Germany), cross-sections of the goods were acquired. Samples were frozen in the cryochamber for two hours at -20°C after being immersed in freezing media (Tissue-Tek®, Leica Microsystems, Ger-man). High profile was used to segment frozen blocks at a thickness of 5 μm.
carbon blades, as detailed in Section 2.9 (EMSCD500, Leica Microsystems, USA).
2.7. Epifluorescence microscopy (EFM) with scanning electron microscopy (SEM). A JSM-6390LV microscope (JEOL, USA) was used to perform scanning electron microscopy with an accelerating voltage of 10 kV. Prior to SEM, samples were covered with a thin layer of gold. An epifluorescence microscope (Bx41, Olympus, USA) fitted with a red filter (excitation = 510–550 nm, emission = 590 nm) was used to conduct fluorescence investigations.
2.8. Evaluation of Coating Film Mechanical Properties. With a 300 N loading cell, a texture analyzer (TA.HD Plus, Stable MicroSystems, UK) was used to evaluate the mechanical characteristics of coating films. The ASTM standard method D882 was used to calculate the percentage of elongation at breakpoint [25]. Using a scalpel (n=5), coating films were carefully removed from the coated pellets' surface. They were then put on the apparatus's extension grips and stretched uniaxially (50 mm/min) until they broke.

2.9. The separation of microspheres from pellets and their subsequent disintegration. The reciprocating cylinder device BioDis RRT10 (Erweka, Germany) was used to assess the microspheres' separation from the pellet surface and subsequent disintegration in the aqueous medium (n=6). The medium was 250 mL of 0.1 N HCl solution (pH 1.2) at 37°C. A total of 20 dips into the aqueous medium were performed on 1 g of pellets that were held inside the dipping tubes by 50 m meshes. To measure the concentration of microspheres separated from the pellets using K-Cell® chambers (Section 2.5) and their average particle size by laser diffraction (Section 2.12), an aliquot was taken after every two immersions.

2.10. Analysis of Laser Diffraction Particle Size. Using an aqueous sample dispersion unit (Hydro 2000SM, Malvern, UK) and MasterSizer 2000 laser diffraction equipment (Malvern, UK), the particle size distribution was ascertained. The Fraunhofer diffraction model was used to derive the results, and the

2.14 Analysis of HPLC. Chlorogenic acid (CGA), a chemical marker of C. glaziovii preparations, was measured using chromatographic analysis. A PerkinElmer Series 200 chromographer was used in conjunction with a previously approved technique [20]. A Luna C18 column (5 m, 150 x 4.6 mm, 100 A˚; Phenomenex, USA) used as the stationary phase. Acetonitrile and trifluoroacetic acid 0.05% (v/v) at a ratio of 11:89 (1 mL/min) made up the mobile phase. Quantification was carried out at 320 nm by comparing the samples with a CGA primary standard curve (1 – 200 μg/mL) after they were injected in duplicate (20 L).

2. Findings and Conversation
2.1. Finding the Best Coating Factors. PLGA microspheres loaded with C. glaziovii exhibited a specific surface area of 1.85 0.01 m2/g and a mean particle size (D4,3) of 4.59 0.04 m. These microspheres should exhibit reduced flowability based on the particle size distribution, as shown by the angle of repose, Hausner ratio, and Carr's index (Section 3.4).

The commercially available material was sieved to separate a fraction of the microcrystalline cellulose pellets (850–1000 m), yielding a weight yield of 74%. Since a monodisperse material results in more homogeneity in the thickness and coverage of coating layers, this fraction, known as "carrier pellets," was used in subsequent tests to lessen the impact of the pellet size distribution on the coating outcome [27]. Two polymers were combined in three concentrations for coating investigations using an IV-Optimal factorial design (Table 2). Total coated surface values were found to be between 20.0 and 99.1% within the experimental domain. When colored coatings are used, RGB analysis has been shown to be sufficient for evaluating the entire coated surface. To the best of the authors' knowledge, coating analyses in pharmaceuticals have not yet employed this technique, which was previously employed as a research tool in food science [22]. As the coated surface expanded, coating solutions containing methylene blue displayed RGB histograms with rising blue frequencies. According to the Supplementary Figure

average diameters of corresponding volumes (D)

4, 3

were established

When compared to S1 (supplementary materials), the RGB histograms produced for coated formulations are significantly different.

(n = 20). The actual particle density was used to compute specific surface area (Section 2.7).

2.11. Studies of Release. Using the paddle method (USP-2 Apparatus model 299, Nova E´tica, Brazil) at 75 rpm, drug release profiles were acquired. Phosphate buffer solution (900 mL, pH 6.8) at 37°C served as the dissolving media. Aliquots were taken at predetermined intervals from the microsphere-coated pellets and freeze-dried microspheres that were positioned at the bottom of the dissolution vessels (n=6). To ascertain the cumulative percentage release of the model drug, samples were centrifuged and subjected to high pressure liquid chromatography (HPLC) analysis (Section 2.14.). The similarity factor (f2, DDSolver software) was used to compare profiles [26].

with uncoated carrier pellets, enabling the differential comparison of RGB pixel frequencies to quantify the coated surface.
According to the findings of the ANOVA, the total coated surface was impacted by variables A (polymer type; p=0.0014), B (polymer concentration; p=0.0004), and C (coating suspension to pellets ratio; p=0.0001). A dependent behavior between polymer type and concentration (interaction AB) and between polymer concentration and coating suspension to pellets ratio (interaction BC) was also indicated by the statistical significance of interactions AB (p=0.0282) and BC (p=0.0023). This response's mathematical model was statistically significant (p 0.0001). The model's prediction R2 (0.9484), adjusted R2 (0.9795), and R2 (0.9914) were all strong indicators of how well the experimental and theoretical

TABLE 2: Total coated surface values as a function of polymer type, concentration, and ratio.

Factors				
#	(A) Polymer type	(B) Polymer concentration (% w/v)	(C) Coating suspension to pellets ratio (mL/g)	Total coated surface (%)
1	Kollidon® VA64	2.5	1:1	26.3
2	Kollidon® VA64	2.5	2:1	65.4
3	Kollidon® VA64	1.0	1:1	26.8
4	Kollidon® VA64	5.0	3:1	82.9
5	Kollicoat® Protect	2.5	2:1	86.9
6	Kollicoat® Protect	2.5	1:1	30.3
7	Kollidon® VA64	5.0	1:1	20.0
8	Kollicoat® Protect	5.0	1:1	26.1
9	Kollidon® VA64	2.5	2:1	63.1
10	Kollicoat® Protect	5.0	2:1	55.7
11	Kollicoat® Protect	2.5	2:1	85.2
12	Kollicoat® Protect	1.0	2:1	88.2
13	Kollidon® VA64	1.0	3:1	93.3
14	Kollidon® VA64	5.0	2:1	51.2
15	Kollicoat® Protect	1.0	3:1	99.1
16	Kollicoat® Protect	2.5	3:1	90.1
17	Kollidon® VA64	1.0	2:1	90.7
18	Kollicoat® Protect	1.0	1:1	27.9
19	Kollicoat® Protect	5.0	3:1	91.0
20	Kollidon® VA64	2.5	3:1	74.7

dataset. The equation describing the response as a function of the relevant coded terms and their coefficients is

$$Coated\ surface\ (\%) = 62.49 - 3.91A + 8.50B\ [1]$$

$$- 0.52B\ [2] - 36.24C\ [1]$$

$$+ 10.21C\ [2] + 3.18AB\ [1]$$

the solution's total viscosity [29]. Lower surface coverage results from the droplets' decreased spreadability. Because the polymer was diluted and there was more coating suspension available to cover the whole surface of the carrier pellets, the effect of viscosity was eliminated when a 3:1 ratio (coating suspension (mL) to pellets (g)) was used. Adjusting the ratio to 1:1 or 2:1 resulted in a decrease in the

$$[2] - 3.97AB\ [1] - 7.39B\ C\ [1] + 2.58B\ [2]\ C\ [1] + 8.24B\ [1]\ 3.02B\ [2]\ C\ [2] + C\ [2]$$

(3) complete coated surface, since there wasn't enough coating to cover the pellets' whole surface. In conclusion, Figure 2 illustrates that the optimal coating conditions (90 percent covered surface) were achieved by using a 2:1 or 3:1 (mL/g) coating suspension to pellets ratio and a low polymer content of 1%. Even though the outcomes of the two ratios were comparable, the 2:1 ratio is a better choice because of the decrease in the When compared to Kollidon® VA64, Kollicoat® Protect often had greater percentages of coated surfaces (Figure 2). Given that it could have a detrimental impact on coating efficiency, this effect might be linked to the viscosity of each polymer solution [28]. However, in comparison to the other terms

(3), the coefficients for all terms considering polymer type were not high. However, the response was significantly influenced by the concentration of the polymer. As the quantity of polymers rose, the percentage of coated surfaces decreased (Figure 2). In this instance, coating suspension droplets created during atomization get bigger when the polymer's concentration rises because of an increase in coating time, lowering the overall cost of processing. Because of its high water solubility, biocompatibility, low moisture-permeability, less requirement for plasticizer, and enhanced mechanical strength, Kollicoat® Protect appears to be a more sensible polymer option [30, 31].
1.1. Fourier Transform Infrared Spectroscopy with Attenuated Total Reflectance (ATR-FTIR). ATR-FTIR was used to track the molecular interactions between the coated polymers and blank PLGA microspheres. Given the potential influence of molecular interactions on the mechanical characteristics of polymers, this evaluation is particularly pertinent [27]. Products that contained extract from C. glaziovii were not evaluated because

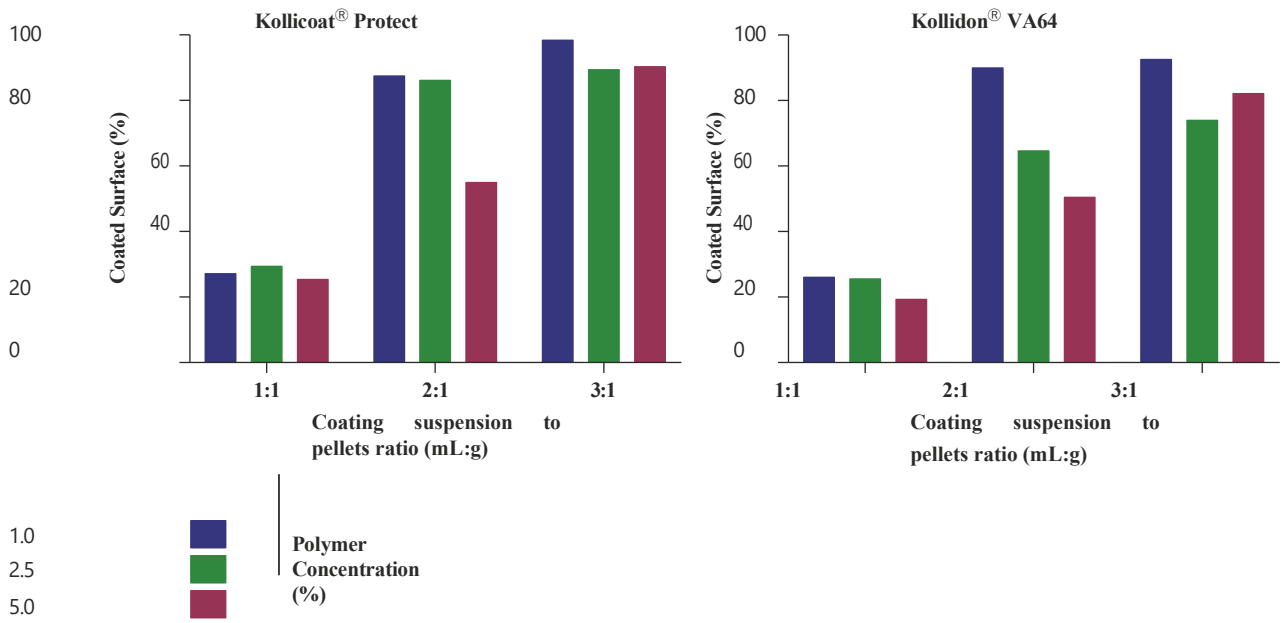

FIGURE 2: Bar graphs correlating the percentage of coated surface to polymer type, polymer concentration, and coating suspension to pellets ratio.

their inability to properly and definitively analyze ATR-FTIR spectra due to their chemical complexity. However, Supplementary Figure S2 presents a representative spectrum of the C. glaziovii extract. Weak OH stretching (3700–3300 cm−1) and -CH stretching (3000–2900 cm−1) bands were visible in the spectrum of PLGA microspheres. Additionally, the lactic-co-glycolic acid chains of PLGA were represented by strong bands for C=O (1751.6 cm−1) and C-O stretching (1500–1000 cm−1). The coated films spectra showed no signs of dislocation or loss of the PLGA microsphere characteristic bands (Figure 3). The spectra for both polymers really just overlapped the spectra of the individual components, suggesting that there were no significant molecular interactions between the coating polymers and microspheres during fluid bed coating. This suggests that the intercalation and trapping of the microspheres within the polymeric layers is the only physical attachment mechanism that kept the particles linked to the coated film.
1.1. Pellets coated with microspheres. As explained in Section 3.1, the ideal coating conditions for

sufficient surface coverage were found to be 1% (w/v) Kollicoat® Protect and a suspension to pellets ratio of 2:1 (mL/g). Under these circumstances, formulations with three coating layers in total were created. 93.7 1.2% was the process yield, which was calculated as the proportion of the experimental mass to the theoretical mass following coating. The microsphere load on the pellet surface was 28.07 1.01 mg/g. In terms of microsphere load, the formulation's yield was 95.6 3.4%, which is consistent with the process's overall yield.

1.2. Analysis of Micromorphology. Spherical features were visible in the SEM of microspheres, and the particle size matched the findings from laser diffraction (Supplementary Figure S3). Carrier pellets (first line, Figure 4)

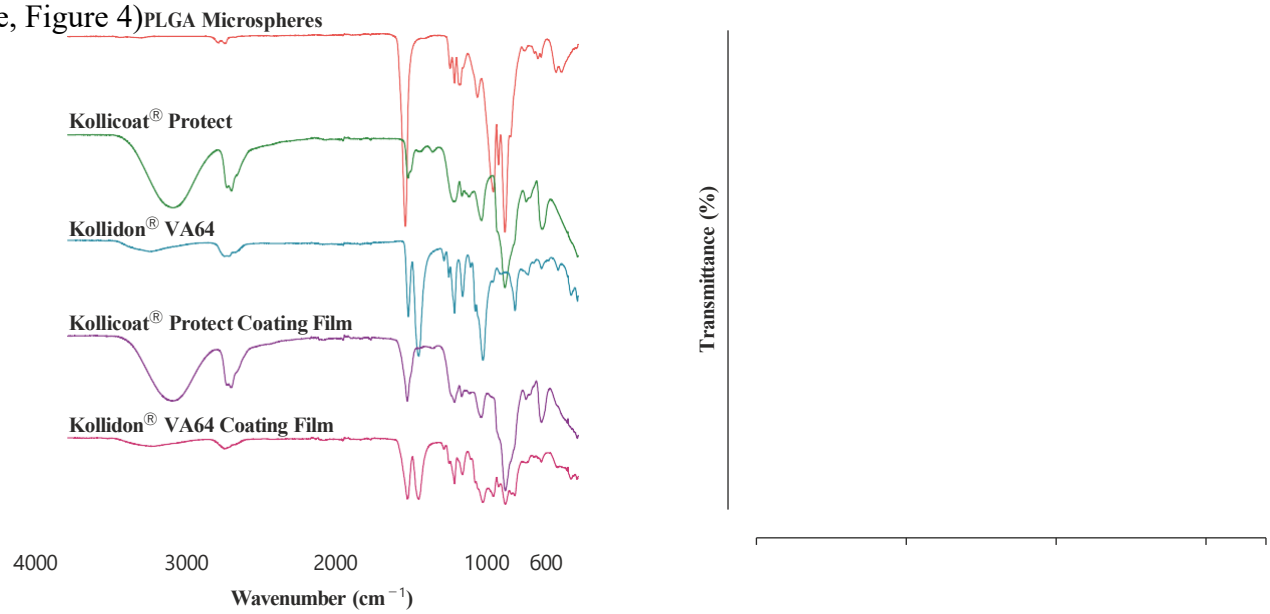

FIGURE 3: ATR-FTIR spectra of blank PLGA microspheres (without *C. glaziovii* extract), polymers, and coating films containing blank PLGA microspheres.

displayed morphological traits that were consistent with those anticipated for normal microcrystalline cellulose pellets. The microcrystalline cellulose particles were superposed during the extrusion-spheronization process, which produced the rough structure that was shown [32]. However, because of the coating polymer, the pellets coated with microspheres had a smoother surface. Additionally, uniformly distributed PLGA microspheres in the polymeric coating film were seen (Figure 4, second line). The dispersion of microspheres on various strata within the polymeric covering was verified by cryosection pictures (Figure 5). This uniform distribution was a clear sign that

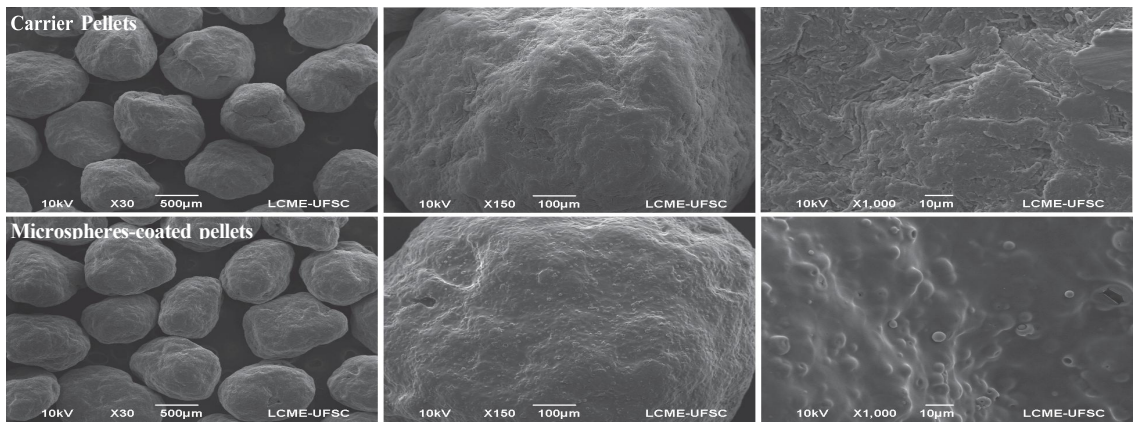

FIGURE 4: SEM micrographs of carrier pellets (**first row**) and microspheres-coated pellets (**second row**) at 30, 150, and 1000x magnification (first, second, and third column, respectively).

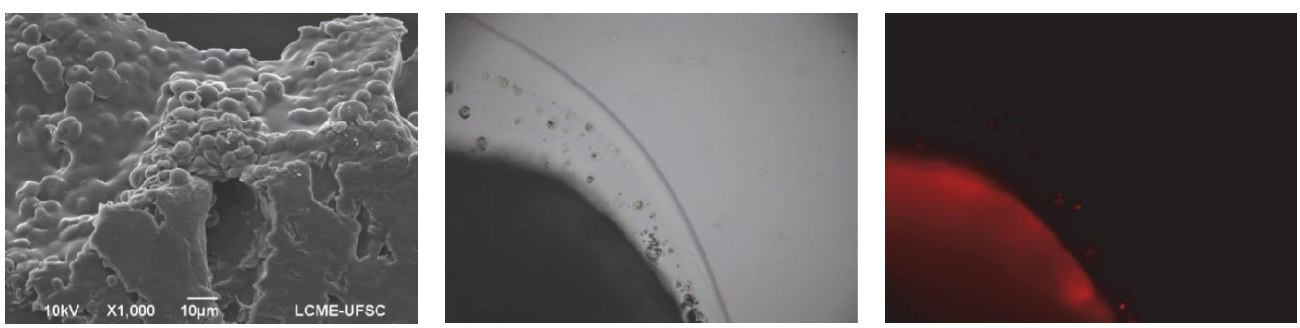

(a) (b) (c)

FIGURE 5: (a) SEM micrograph of the cryosectioned microspheres-coated pellets (1000x). Micrographs of the cryosectioned microspheres-coated pellets under (b) light and (c) epifluorescence microscopy (40x magnification).

agglomeration did not occur during the coating process, and the polymer concentration was adequate to maintain indi- vidual microparticles separated from each other after drying. Such findings are relevant as the drying process leads to the shrinkage of the coating layer as water is removed, reducing the distance between the dispersed particles. If the interparticle distance is too short (if not enough polymer is used), particles may agglomerate, potentially impairing their ability to be released from the coating film in a dispersed state. Epifluorescence microscopy (EFM) showed *C. glaziovii* freeze-dried extract particles displayed intense fluorescence signal (Supplementary Figure S4), which can be attributed to the high content of phenolic compounds of the extract [33]. Consequently, *C. glaziovii*-loaded PLGA microspheres also displayed fluorescence signal under EFM. Cryosectioned pellets clearly displayed the polymeric layer around the microcrystalline cellulose core (Figure 5(b)), with fluorescent particles dispersed within it (Figure 5(c)). Also, a disperse fluorescence signal was noticed in parts of the polymeric film.

It is hypothesized that this could be caused by the early release of the extract from the microspheres during the coating process. This effect may be attributed to the coating process itself, as the microspheres are maintained under constant stirring in aqueous medium, potentially fostering partial release of the extract. As the coating layer dried, the extract also solidified, potentially causing the diffuse fluorescent signal observed. A set of EFM micrographs is provided as supplementary data (Supplementary Figures S5 and S6).

1.1. Densities and Flowability. A threefold decrease was noticed on the average bulk density when comparing the freeze-dried extract with extract-loaded PLGA microspheres (p 0.0001, Table 3). The reduction on bulk density means an equal mass of the product will occupy a higher volume, therefore reducing the total dose that can be compressed into tablets or encapsulated in gelatin capsules. In general, reduction of the total dose is undesired, especially when high

TABLE 3: Densities and flow-indicative parameters of the products.

Parameters	*C. glaziovii* extract	Microspheres	Carrier pellets	Coated pellets
Bulk density (g/cm³)	0.31 ± 0.01	0.11 ± 0.01	0.69 ± 0.02	0.74 ± 0.03
Tapped density (g/cm³)	0.40 ± 0.02	0.21 ± 0.01	0.74 ± 0.01	0.78 ± 0.02
True density (g/cm³)	1.564 ± 0.002	1.461 ± 0.001	1.499 ± 0.001	1.571 ± 0.005
Hausner ratio	1.27 ± 0.02	1.81 ± 0.01	1.05 ± 0.01	1.03 ± 0.01
Carr's index (%)	21.0 ± 1.4	44.7 ± 0.2	5.3 ± 1.0	11.8 ± 0.8
Angle of repose (°)	37.8 ± 1.4	48.4 ± 1.3	20.9 ± 0.6	14.5 ± 0.3

dosages are needed to achieve drug therapeutic concentra- tions in blood. On the other hand, a high bulk density was found for the microspheres-coated pellets. No significant differences between carrier and coated pellets were noticed (p 0.05).

Regarding tapped density, a similar behavior was noticed. *C. glaziovii* extract had an increase in density after com- paction of around 30%. Meanwhile, extract-loaded micro- spheres displayed an increase in density of around 90%. This difference is indicative of the increased interparticle forces that act on the microstructured system. These forces are responsible for maintaining the individual particles separated from each other, reducing the bulk density and increasing the difference between bulk and tapped densities of the material [7]. Carrier and coated pellets showed no relevant differences between their bulk and tapped densities.

True density results showed *C. glaziovii* extract has a denser particle structure when compared with *C. glaziovii*- loaded microspheres. Microspheres-coated pellets also showed denser structure when compared to their uncoated form due to the addition of the polymeric coating layer, which increases the density and decreases the porous network of the system.

Hausner ratio and Carr's index values were assessed as indicative of the flowability of the products. As previously discussed, the difference between these densities is related to the interparticle forces acting on the particulate system [7, 8]. Since it is known that the interparticle forces also influence flow, these density values can be used to estimate the flowability of the products. Freeze-dried *C. glaziovii* extract showed unsatisfactory results for both parameters, indicating poor flowability. The encapsulation of the extract in PLGA microspheres, though advantageous in many biopharmaceu- tical aspects, led to a product with even poorer flowability. The reduction in flowability was directly related to the smaller particle size of the microspheres when compared with the original particle size of the freeze-dried extract (Supplemen- tary Figure S4). On the other hand, carrier pellets, as well as microspheres-coated pellets, showed excellent indexes, indicating free-flowing properties.

The angle of repose, which is a much more reliable indicative measure of flowability, showed similar results. *C. glaziovii* extract (37.8 1.4°) and microspheres (48.4 1.3°) were characterized as poor-flowing powders. The repose pile formed by the microspheres displayed an irregular shape (Figure 6(b)), characteristic of products exhibiting extreme resistance to flow. In contrast, microspheres-coated pellets showed free-flowing properties (14.5 ± 0.3°) and a broadrepose pile (Figure 6(d)). Therefore, it is concluded that the association of poorly flowing microspheres to pellets is a great alternative towards providing free-flow to the product.

1.2. Mechanical Properties of the Coating Films. Texture analyses of the coating films, with and without microspheres, showed that the incorporation of microspheres to the coating solution led to a less flexible film (p 0.0001). The elongation at breakpoint for Kollicoat® Protect film obtained under optimized conditions but without microspheres was 37.4 2.5%. Meanwhile, the elongation at breakpoint for the microspheres-coated pellets' film was only 21.5 3.2%. The elongation at breakpoint is an important parameter regarding flexibility of films because it is indicative of the ability of the film to deform before breaking. The addition of microspheres to the coating solution led to the formation of a weaker and less flexible coating, likely due to the discontinuity of the coating layers, caused by the interposition of the particles within. This result is corroborated by the ATR-FTIR results (Section 3.2.), which indicated that no molecular interactions occurred between the polymeric film and PLGA micro- spheres. If strong molecular interactions took place, a dif- ferent mechanical behavior would be more likely, giving rise to a stronger film, with potentially higher elongation at breakpoint.

1.3. Microspheres Detachment from Pellets and Subsequent Disaggregation. Detachment of microspheres from the sur- face of the coated pellets was assessed using a reciprocating cylinder

apparatus. In general, detachment occurred quickly (Figure 7, top left graph). It is assumed that the polymer read- ily dissolved in contact with the aqueous medium, releasing the particles. Laser diffraction analysis showed microspheres immediately detached back to their original average particle size when compared with the coating suspension prior to fluid bed coating (Figure 7, top right graph). On the other hand, freeze-dried microspheres (prior to redispersion and coating) took much longer to disaggregate when compared with those microspheres detached from the coated pellets. The instantaneous disaggregation of the particles is a result of their homogeneous disperse state in the polymeric coating film, as shown by the SEM micrographs (Figures 4 and 5(a)). When the polymer dissolved, particles instantly detached back to their original particle size, as shown by the schematic representation in Figure 7 (bottom). The aforementioned results showcase the potential of this technique in improving the redispersibility of polymeric microspheres.

FIGURE 6: Repose piles obtained for the (a) *C. glaziovii* extract, (b) *C. glaziovii*-loaded PLGA microspheres, (c) carrier pellets, and (d) microspheres-coated pellets.

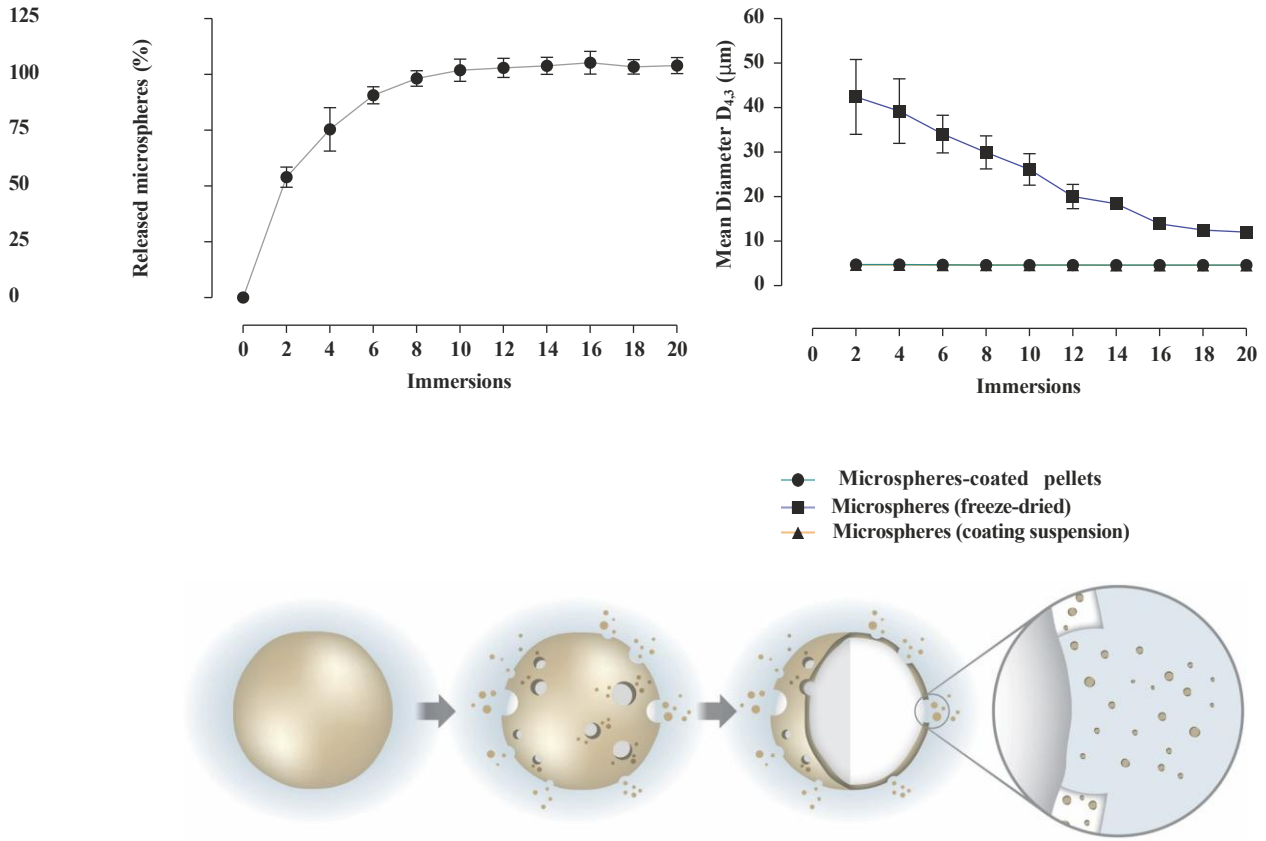

FIGURE 7: (**Top**) Plots correlating the number of immersions to the percentage of detached microspheres from the coated pellets (left graph) and to the average diameter of the particles (right graph; note: lines for microspheres-coated pellets and suspended microspheres overlapped). (**Bottom**) Schematic representation of the behavior of microspheres-coated pellets in contact with aqueous media. Coating polymer readily dissolves releasing disaggregated microspheres.

1.4. Release Studies. *In vitro* release studies were carried out to verify if the attachment of PLGA microspheres to the surface of pellets by fluid bed coating led to relevant changes in drug release profile. Chlorogenic acid, a major constituent of *C. glaziovii* extracts, was monitored by HPLC to determine the cumulative release of the marker from the microspheres. Figure 8 shows the release profiles obtained. It is noticeable that the microspheres themselves were able to prolong the release of chlorogenic acid when compared with the disso- lution profile of the freeze-dried extract (similarity factor f_2

1.5. = 7).

Release profiles of the chemical marker from micro- spheres prior to and after the fluid bed coating showed very similar rate and extent ($f_2 = 48$). However, microspheres released from pellets had a slightly increased burst release effect when compared with unprocessed microspheres. The burst release could be related to the early release of the vegetal extract in the coating suspension during fluid bed processing. As shown by the EFM micrographs (Figure 5(c)), it seems that a small amount of free extract was dispersed in the polymer coating layer, outside of the microspheres. When the polymer dissolved, the free extract may dissolve as

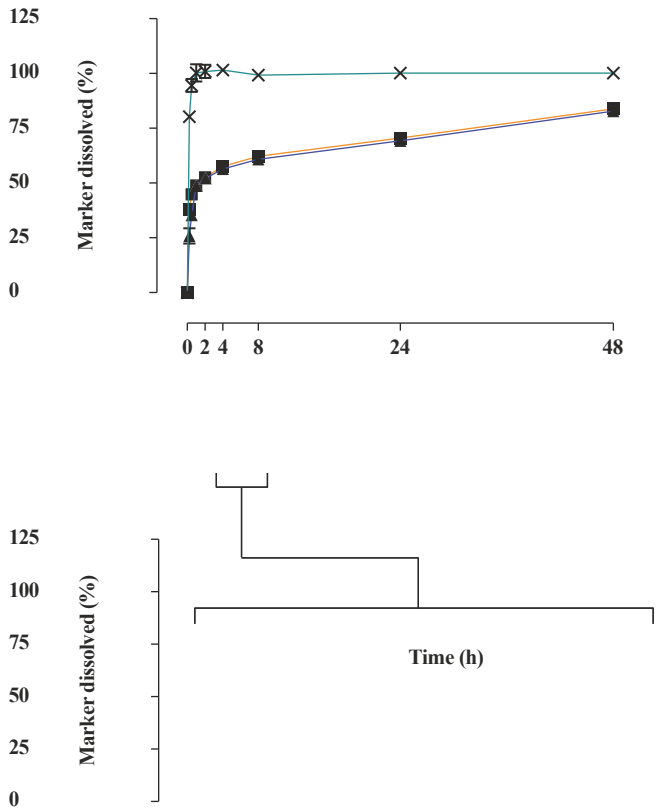

enhance flowability. However, the inner compartment is likely to impact the product performance of the nanoparti- cles, and therefore it would not be appropriate for a "fast- release" system. Following similar principles, a proprietary technique to associate two particle populations (one nano- sized and another microsized) has been proposed [9]. Also, a variety of nanocomposite systems have been suggested. Clay and carbon nanotubes have been successfully transformed into nanocomposites, where nanoparticles were coated onto the surface of polymeric spheres by ball-milling process [10]. A drug delivery vehicle comprising a carrier particle bearing drug microparticles on its surface has also been investigated [13], whereas the deposition technology relied on sublimation.

More applicable techniques such as spray drying and electrostatic coating have also displayed promising results for this application. For instance, spray drying of amorphous drug nanoparticles with lactose generated a matrix-like structure that displayed fast-dissolving properties [35]. Alternatively, core-shell-like structures can be obtained by spray drying drug particles concurrently with silica particles [35]. The manufacturing of redispersible granules containing TiO_2 nanoparticles has also been described using the spray drying technique, leading to stable 20 to 50 μm spherical granules [36]. TiO_2 nanoparticles have also been associated with the surface of plastic granules using a combination of an electrostatic adhesion and heat treatments [37].

Nonetheless, as far as the authors are concerned, none of these current technologies are as simple and easy to imple- ment as the standard method developed in this study.

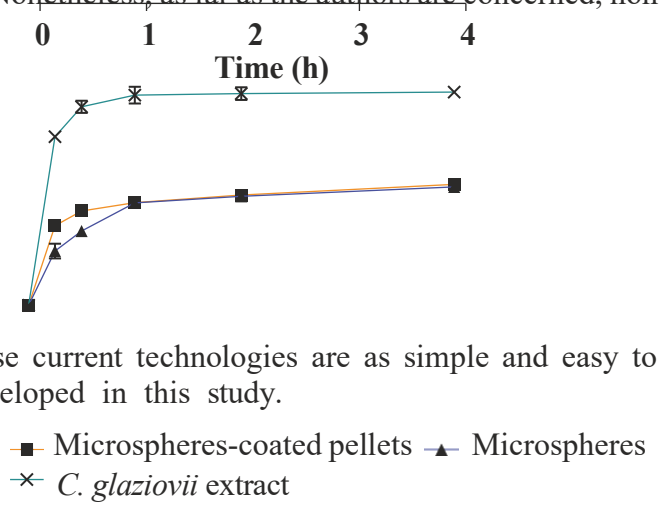

FIGURE 8: *In vitro* chlorogenic acid (chemical marker) release pro- files from microspheres, microspheres-loaded pellets, and freeze- dried *C. glaziovii* extract.

well, leading to the pronounced burst release effect observed. Faster disaggregation of microspheres after detachment from the surface of the pellets can also contribute towards the burst release effect by allowing faster release of the model drug entrapped.

1.6. Comparison with Other Strategies to Promote Flow Enhancement. Promoting flow enhancement to micrometric and submicrometric particles is of high importance for industrial applications. The general understanding in the industrial pharmacy field is that transforming small parti- cles into multiparticulate systems (e.g., wet/dry granulation, extrusion-spheronization) is the most viable alternative to solve flowability issues [34]. These strategies are valuable for regular powder mixtures but may be inadequate for mul- tifunctional particles such as drug-loaded microspheres. Under these situations, alternative methods such as the proposed herein can be much more advantageous.

For instance, a modified pellet formulation has been proposed before containing an inner matrix layer of nanopar- ticles [12]. Potentially, the large particle size of pellets canPelletization and wet/dry granulation technologies are too aggressive on the nanoparticle's structure and often lead to products

that do not disintegrate and/or release their contents as fast as would be desirable. Spray drying may lead to particulate products that are still too small to display optimal flow properties. Therefore, the top-spray polymeric coating on carrier pellets technology as proposed here can be an ideal alternative to combine nano/microstructures with larger particles (millimetric range) with the goal of improving flowability and redispersibility without impairing product performance.

2. Conclusion

A novel approach with the goal of improving the flow proper- ties and redispersibility of micro- and submicrometric parti- cles was assessed, targeting the production of an industrially- viable particulate product. Poorly flowing PLGA micro- spheres containing a model vegetal extract were successfully associated with pellets by fluid bed coating employing the polymer Kollicoat® Protect. An excellent improvement of the flow properties of the product was achieved. Microspheres readily detached from the surface of the pellets into the aqueous medium, without aggregation and with minimal interference on the release profile (rate and extent) of the chemical marker.

The methodology proposed is suitable for the associa- tion of different types of micrometric and submicrometric particles when an improvement of the overall flowabilityand redispersibility is desired. Based on our results, we expect this methodology can be expanded to other systems besides microspheres (e.g., polymeric nanoparticles). This approach is considered easily scalable and economically- viable as the equipment needed for fluid bed coating is already used in the manufacture of solid dosage forms, potentially reducing implementation costs. The association of nano/microstructures to pellets may become a viable solution to common issues related to the lack of flow and redispersibil- ity in dried pharmaceutical particulate systems.

Supplementary Materials

Supplementary Materials provided online include 6 sup- plementary figures. RGB color histograms of uncoated and coated pellets (Supplementary Figure S1). Represen- tative ATR-FTIR spectrum of *C. glaziovii* freeze-dried extract (Supplementary Figure S2). Scanning electron micro- graph of *C. glaziovii* microspheres (Supplementary Fig- ure S3). Light and epifluorescence micrographs of *C. glaziovii* extract (Supplementary Figure S4). Cross-sectioned microspheres-coated pellets (Supplementary Figures S5 and S6). *(Supplementary Materials)*

References

[1] "Design and evaluation of novel pH-sensitive chitosan nanoparticles for oral insulin delivery," European Journal of Pharmaceutical Sciences, vol. 42, no. 5, pp. 445–451, 2011, by A. Makhlof, Y. Tozuka, and H. Takeuchi.

[2] A. A. Velasquez, L. M. Ferreira, M. F. L. Stangarlin, C. D. B. Da Silva, C. M. B. Rolim, and L. Cruz, "New Pullulan–Eudragit® S100 blend microparticles for oral delivery of risedronate: formulation, in vitro assessment, and tableting of blend microparti-cles," Materials Science and Engineering C: Materials for Biological Applications, vol. 38, no. 1, pp. 212–217, 2014.

[3] "Stability study and in-vivo evaluation of lornoxicam loaded ethyl cellulose microspheres," International Journal of Pharmaceutical Sciences and Drug Research, vol. 6, pp. 26–30, 2014, L. K. Tyagi and M. L. Kori.

Nanoparticle multilayers: Surface modification of photosensitive drug microparticles for enhanced stability and in vitro bioavailability, Journal of Nanoscience and Nanotechnology, vol. 6, no. 9-10, pp. 3252–3260, 2006; N. Li, D. S. Kommireddy, Y. Lvov, W. Liebenberg, L. R. Tiedt, and M. M. De Villiers.

[5] "Dry particle coating to improve the flowability of cohesive powders," Powder Technology, vol. 158, no. 1-3, pp. 21–33, 2005; J. Yang, A. Sliva, A. Banerjee, R. N. Dave, and R. Pfeffer.
[6] A Guide to Pharmaceutical Particulate Science, Taylor & Francis, London, UK, 2003; A. J. Hickey, T. M. Crowder, M. D. Louey, and N. Orr.
The physics of powder flow: Applied to pharmaceutical solids, by T. M. Crowder and A. J. Hickey, Pharmaceutical Technology, vol. 24, no. 2, pp. 50–58, 2000.
[8] Q. Li, V. Rudolph, B. Weigl, and A. Earl, "Interparticle van der Waals force in powder flowability and compactibility," International Journal of Pharmaceutics, vol. 280, no. 1-2, pp. 77–93, 2004.
[9] "Method of making positions including particles," M. P. Shinbach and J. R. Baran, 3M Innovative Properties, US20080152913A11, 2008.
[10] "Composites," by D. Mao and Z. Yaniv, Applied Nanotech Holdings, WO2010104710A1, 2010.
In their paper "Medicinal coating based on a mixture of solid lipidic nanoparticles and polymers," G. D. Quintanar, R. F. A. Ganem, O. E. A. Camacho, et al. MX2010005803A, UNAM Universidad Nacional Autonomous de Mexico, 2011.
[12] "Mul-tiparticulate form of administration, comprising nucleic acid-containing mucoadhesive active ingredients, and method for producing said form of administration," by R. Lizio, H.-U. Petereit, D. Trupti, and M. Gottschalk US8568778B2, Evonik Ro¨hm Gmbh, 2013.
[13] "Drug microparticles, processes of preparing them and a drug delivery vehicle comprising them," Teva Pharmaceutical Industries Ltd., US8663703B2, 2014; E. I. Lerner, V. Rosenberger, M. Flashner-Barak, A. Drabkin, and N. Moldavski.
[14] Powder Technology, vol. 189, no. 3, pp. 409–415, 2009; E. Emery, J. Oliver, T. Pugsley, J. Sharma, and J. Zhou, "Flowability of moist pharmaceutical powders."
[15] "In vivo potential hypoglycemic and in vitro vasorelaxant effects of Cecropia glaziovii standardized extracts," Brazilian Journal of Pharmacognosy, vol. 25, no. 5, pp. 473–484, 2015; D. P. Arend, T. C. dos Santos, L. H. Cazarolli et al.
[16] S. Delarcina, M. T. R. Lima-Landman, C. Souccar, R. M. Cys-neiros, M. M. Tanae, and A. J. Lapa, "Inhibition of histamine-induced bronchospasm in guinea-pigs treated with Cecropia glaziovii Sneth. extracts and correlation with the in vitro activity in tracheal muscles," Phytomedicine, vol. 14, no. 5, pp. 328–332, 2007.
[17] ACE activity during the hypotension caused by standardized aqueous extract of Cecropia glaziovii Sneth: A comparative research to captopril effects in rats, Phy-tomedicine, vol. 14, no. 5, pp. 321–327, 2007. M. F. M. L. Ninahuaman, C. Souccar, A. J. Lapa, and M. T. R. Lima-Landman.
[18] Anxiolytic-like actions of Cecropia glaziovi Sneth. in mice: an evaluation by F. F. Rocha, A. J. Lapa, and T. C. M. De Lima, Pharmacology Biochemistry & Behavior, vol. 71, no. 1-2, pp. 183–190, 2002. Phytomedicine, vol. 14, no. 6, pp. 396–402, 2007; F. F. Rocha, M. T. R. Lima-Landman, C. Souccar, M. M. Tanae, T. C. M. De Lima, and A. J. Lapa, "Antidepressant-like effect of Cecropia glazioui Sneth. and its constituints – In vivo and in vitro characterization of the underlying mechanism."
[20] Response Surface Methodology IV-Optimal design applied to the performance improvement of an RP-HPLC-UV, A. O. Beringhs, M. Dalmina, T. B. Creczynski-Pasa, and D. Sonaglio
technique for measuring phenolic acids in Cecropia glaziovii products, Brazilian Journal of Pharmacognosy, vol. 25, no. 5, pp. 513–521, 2015.
[1] "Technological development of Cecropia glaziovi Snetl. extract pellets by extrusion-spheronization," Brazilian Journal of Pharmacognosy, vol. 23, no. 1, pp. 161–168, 2013, A. O. Beringhs, F. M. Souza, A. M. de Campos, H. G. Ferraz, and D. Sonaglio.
[2] "Prediction of compositional and sensory characteristics using RGB digital images and multivariate calibration techniques," Analytica Chimica Acta, vol. 706, no. 2, pp. 238–245, 2011, G. Foca, F. Masino, A. Antonelli, and A. Ulrici.

[3] R. L. Carr, "Evaluating flow properties of solids," Chemical Engineering, vol. 72, no. 2, pp. 163-168, 1965.
[4] Experimental investigation of the angle of repose of pulverized coal, Particuology, vol. 8, no. 5, pp. 482–486, 2010; W. Wang, J. Zhang, S. Yang, H. Zhang, H. Yang, and G. Yue.
[5] ASTM, "Standard test method for tensile properties of thin plastic sheeting. D882," Annual Book of American Standard Testing Methods, 2002.
[6] "DDSolver: An add-in program for modeling and comparison of drug dissolution profiles," (Y. Zhang, M. Huo, J. Zhou, et al.), The AAPS Journal, vol. 12, no. 3, pp. 263–271, 2010.
[7] Aqueous Polymeric Coatings for Pharmaceutical Dosage Forms, J. W. McGinity and L. A. Felton, Informa Healthcare, London, UK, 3rd edition, 2008.
[8] E. Teunou and D. Poncelet, "A review and state of the art on batch and continuous fluid bed coating," Journal of Food Engineering, vol. 53, no. 4, pp. 325–340, 2002.
[9] "Top-spray fluid bed coating: Scale-up in terms of relative droplet size and drying force," Powder Technology, vol. 184, no. 3, pp. 318–332, 2008, P. D. Hede, P. Bach, and A. D. Jensen.
[10] "Film coatings for taste masking and moisture protection," International Journal of Pharmaceutics, vol. 457, no. 2, pp. 395–406, 2013, S. Joshi and H.-U. Petereit.
[11] "Design and evaluation of bilayered buccal film preparations for local administration of lidocaine hydrochloride," edited by M. Preis, C. Woertz, K. Schneider, and others, European Journal of Pharmaceutics and Biopharmaceutics, vol. 86, no. 3, pp. 552–561, 2014.
[12] "Physicochemical properties of granulating liquids and their influence on microcrystalline cellulose pellets obtained by extrusion-spheronization technology," International Journal of Pharmaceutics, vol. 291, no. 1-2, pp. 99–111, 2005; R. Dreu, J. Sˌirca, K. Pintye-Hodi, T. Burjan, O. Planinˌsek, and S. Srčicˇ.
[13] "Study of phenolic compounds as natural antioxidants by a fluorescence method," Talanta, vol. 60, no. 2-3, pp. 609–616, 2003; M. Lopez, F. Martínez, C. Del Valle, M. Ferrit, and R. Luque.
[14] S. Shanmugam, "Technological advancements in granulation techniques and technologies," BioImpacts, vol. 5, no. 1, pp. 55–63, 2015.
[15] Melzig, D. Niedbalka, C. Schilde, and A. Kwade, "Spray drying of amorphous ibuprofen nanoparticles for the production of granules with enhanced drug release," Colloids and Surfaces A: Physicochemical and Engineering Aspects, vol. 536, pp. 133–141, 2018.
[16] "Spray drying of TiO2 nanoparticles into redispersible granules," Powder Technology, vol. 203, no. 2, pp. 384–388, 2010, B. Faure, J. S. Lindelov, M. Wahlberg, N. Adkins, P. Jackson, and L. Bergstrom.
The study "Coating TiO2 nanoparticles on the surface of transparent plastic granules using combined electrostatic and heating" (Sutisna, M. Rokhmat, E. Wibowo, Khairurrijal, and M. Abdul-lah)

techniques to degrade organic pollutants in water using photocatalysis," Environmental Nanotechnology, Monitoring and Management, vol. 8, pp. 1–10, 2017.